



HAL
open science

Electrochemical Storage of Atomic Hydrogen on Single Layer Graphene

Quanfeng He, Lanping Zeng, Lianhuan Han, Matthew M Sartin, Juan Peng, Jian-Feng Li, Alexander Oleinick, Irina Svir, Christian Amatore, Zhong-Qun Tian, et al.

► **To cite this version:**

Quanfeng He, Lanping Zeng, Lianhuan Han, Matthew M Sartin, Juan Peng, et al.. Electrochemical Storage of Atomic Hydrogen on Single Layer Graphene. *Journal of the American Chemical Society*, 2021, 143 (44), pp.18419-18425. 10.1021/jacs.1c05253 . hal-03551357

HAL Id: hal-03551357

<https://hal.sorbonne-universite.fr/hal-03551357v1>

Submitted on 1 Feb 2022

HAL is a multi-disciplinary open access archive for the deposit and dissemination of scientific research documents, whether they are published or not. The documents may come from teaching and research institutions in France or abroad, or from public or private research centers.

L'archive ouverte pluridisciplinaire **HAL**, est destinée au dépôt et à la diffusion de documents scientifiques de niveau recherche, publiés ou non, émanant des établissements d'enseignement et de recherche français ou étrangers, des laboratoires publics ou privés.

Electrochemical Storage of Atomic Hydrogen on Single Layer Graphene

Quanfeng He¹, Lanping Zeng¹, Lianhuan Han^{1*}, Matthew M. Sartin¹, Juan Peng², Jian-Feng Li¹, Alexander Oleinick³, Irina Svir³, Christian Amatore^{1,3*}, Zhong-Qun Tian¹, Dongping Zhan^{1,2*}

¹State Key Laboratory of Physical Chemistry of Solid Surfaces (PCOSS); Fujian Science & Technology Innovation Laboratory for Energy Materials of China; Engineering Research Center of Electrochemical Technologies of Ministry of Education; Department of Chemistry, College of Chemistry and Chemical Engineering; and Department of Mechanical and Electrical Engineering, School of Aerospace Engineering, Xiamen University; Xiamen 361005, China.

²Department of Chemistry, College of Chemistry and Chemical Engineering, Ningxia University; Yinchuan 750021, China.

³PASTEUR, Département de chimie, École normale supérieure, PSL University, Sorbonne Université, CNRS, 75005 Paris, France.

ABSTRACT: If hydrogen can be stored and carried safely at high density, hydrogen-fuel cells offer effective solutions for vehicles. Stable chemisorption of atomic hydrogen on single layer graphene (SLG) seems a perfect solution in this regard, with a theoretical maximum storage capacity of 7.7 wt%. However, generating hydrogenated graphene from H₂ requires extreme temperatures and pressures. Alternatively, hydrogen adatoms can easily be produced under mild conditions by electroreduction of protons in solid/liquid systems. Graphene is electrochemically inert for this reaction, but H-chemisorption on SLG can be carried out under mild conditions via a novel Pt-electrocatalyzed “spillover-surface diffusion-chemisorption” mechanism, as we demonstrate using dynamic electrochemistry and isotopic Raman spectroscopy. The apparent surface diffusion coefficient ($\sim 10^{-5}$ cm² s⁻¹), capacity (~ 6.6 wt%, $\sim 85.7\%$ surface coverage), and stability of hydrogen adatoms on SLG at room temperature and atmospheric pressure are significant, and they are perfectly suited for applications involving stored hydrogen atoms on graphene.

1. INTRODUCTION

Hydrogen is the cleanest fuel with a high energy density, but without the production or emission of carbon dioxide or any other pollutants.¹ However, neither compressed gas nor liquid hydrogen is safe for daily use in mobile applications.² Therefore, sorbent approaches seem to be the best choice for hydrogen storage.^{3,4} Among the possible materials for hydrogen storage, graphene (Gr) is considered to be one of the most promising materials.^{5,6} The storage of hydrogen molecules (H₂) on a Gr surface by physical adsorption requires extreme temperatures and pressures even in the presence of metallic/metal oxide nanoparticles, due to the weak attractive van der Waals forces.^{4,7} In addition, the performance of hydrogen storage on Gr and carbon nanotubes by physisorption is disputed, because of the difficulties in obtaining reproducible adsorption capacity measurements.^{8,9} An alternative way to store atomic hydrogen on Gr is by chemical adsorption based on a spillover mechanism^{10–12}: a catalyst is employed to dissociate hydrogen gas to hydrogen adatoms (H_{ad}), which spill over from the catalyst onto Gr and are stored there.^{13,14} Theoretically, if each carbon atom provides one adsorption site for H_{ad}, the saturated storage capacity of Gr (i.e., surface coverage: 100%) would be 7.7 wt%.¹⁵ However, under solid/gas conditions, high pressure and low temperature^{16–18} are required to enable the disso-

ciation of H₂ even in the presence of catalysts such as platinum (Pt), palladium (Pd), nickel (Ni), metallic alloys or oxides, etc.^{19–23} Therefore, fulfilling this goal in this manner would impose unrealistic conditions for daily use mobile applications.

Relying on electrochemical solid/liquid systems appears to be a more advantageous strategy for producing H_{ad} under ambient conditions, because the H_{ad} source simply consists of the protons (H⁺) present in any acidic, neutral, or alkaline aqueous electrolyte solution. Note that, in this respect, since decarbonized H₂ needs to be produced by electrochemical reduction of protons, and since fuel cells already rely on electrochemical technologies, if such a solution is technically practical, it would even suppress one crucial step since it does not require any need for gaseous hydrogen. However, although carbon materials, including Gr, are inert for electroreduction of H⁺, we demonstrate herein that this problem can be easily overcome. H_{ad} monolayers can be readily electrodeposited and stably adsorbed on single-layer Gr sheets (SLG) under mild conditions through a Pt-electrocatalyzed “spillover-surface diffusion-chemisorption” mechanism. In the following we characterize this mechanism electrochemically and then demonstrate by Raman spectroscopy that H_{ad} atoms are stably stored by chemisorption onto SLGs.

2. EXPERIMENTAL SECTION

Chemicals and Materials. Sulfuric acid (H_2SO_4 , D_2SO_4) was purchased from Sinopharm Group Co. Ltd. and used as received without further purification. Aqueous solutions used in the experiments were prepared with deionized water ($18.2 \text{ M}\Omega\cdot\text{cm}$, Milli-Q, Millipore Co.). Nitrogen gas (N_2 , 99.999%) was purchased from Linde Gas Co., China.

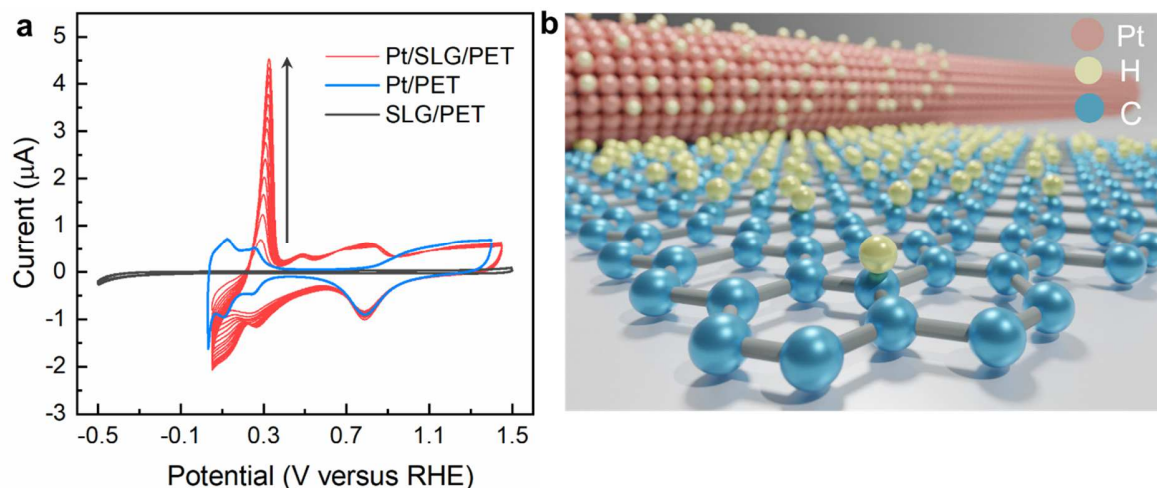


Figure 1. Pt-electrocatalyzed adsorption and desorption of atomic hydrogen on single layer graphene. (a) Cyclic voltammograms of Pt/SLG/PET electrode (red; showing one CV every 20 voltammetric cycles), Pt/PET electrode (blue) and SLG/PET electrode (grey) at 100 mV/s in $0.5 \text{ M H}_2\text{SO}_4$ solution. The dimensions of the SLG flake were $2.1 \text{ mm} \times 1.8 \text{ mm}$. (b) Schematic illustration of electrocatalytic “spillover-surface diffusion-chemisorption” mechanism on Pt/SLG/PET electrode assuming a chemical adsorption of H_{ad} adatoms onto the graphene matrix. (See SI, section S4 for the initial voltammograms performed on a non-activated Pt/SLG/PET electrode.

Graphene sample preparation. SLG was grown via chemical vapor deposition (CVD) on copper foils and then transferred to an approximately $500 \mu\text{m}$ thick polyethylene terephthalate (PET) substrate and SiO_2/Si substrate using wet transfer techniques. The SLG flakes were prepared in two sizes for different purpose of the experiments in order to ensure the best accuracy possible of the measurements. For determination of apparent H_{ad} diffusion coefficient on SLG, $4 \text{ mm} \times 4 \text{ mm}$ rectangular flakes were used in order that SLG loading process through the 3 mm length of the Pt-microwire contact line could be described with classical semi-infinite linear diffusion equation (see Section S1). For measurements of H_{ad} loading capacities, $2.1 \text{ mm} \times 1.8 \text{ mm}$ rectangular SLG flakes were used in order that the number of carbon sites was known with sufficient precision as well as to achieve faster loading times (note in this respect that the exact placement of the Pt-microwire onto the flakes, viz. centered and parallel to either sides, or along one diagonal, did not led to any difference in the maximum loading capacity which kept reproducible).

Electrochemical measurements. A CHI 631B potentiostat (CH Instruments, Inc.) was employed to perform electrochemical experiments at room temperature (298 K) as well as over the temperature range ($284\text{-}303 \text{ K}$) required to determine the activation barrier of the site-exchange process (see Figure 4 and Figure S10). Before each measurement, the electrolyte was pre-saturated with high-purity ni-

trogen (N_2) by bubbling the gas for at least 15 min to eliminate the interference from oxygen (O_2). N_2 gas was flowed continuously into the headspace of the electrolytic cell to maintain the inert gas environment during the measurements. All electrochemical experiments were performed using a three-electrode system, $\text{Hg}/\text{Hg}_2\text{SO}_4$ with saturated K_2SO_4 solution was used as the reference electrode, and a platinum mesh was used as the counter electrode. All potentials (V) were converted to the RHE scale using the follow-

ing formula: $E_{\text{RHE}} = E_{\text{RE}} + 0.65 + 0.059 \times \text{pH}$, where E_{RE} is the potential of $\text{Hg}/\text{Hg}_2\text{SO}_4$ electrode.

Raman characterizations. All of the Raman measurements were performed on Xplora confocal microprobe Raman system (HORIBA Jobin-Yvon) with 532 nm laser excitation, the laser spot was about $2 \mu\text{m}$ using a $50\times$ microscope objective ($\text{NA} = 0.55$). The graphene substrate material used for most electrochemical experiments reported in the main text was PET, but this was not suitable for Raman characterization due to the strong background signals of PET. Therefore, we used SiO_2/Si wafer as the substrate for Raman characterization of graphene. In the deuterium substitution experiment, ultrathin HOPG was used, because SiO_2/Si has a broad and strong background in the low wavenumber region from 780 cm^{-1} to 850 cm^{-1} .

3. RESULTS AND DISCUSSION

A 3-mm -long Pt microwire (diameter: $25 \mu\text{m}$) was tightly inserted and centered between a flake of SLG supported by a PET membrane and a Nafion membrane to construct a well-defined Pt/SLG linear boundary (see Figure S1). The Pt microwire flanks contacting both the aqueous electrolyte and SLG acts as the catalytic zone for electrochemical generation of H_{ad} , and the SLG provides the storage zone for H_{ad} spilling and diffusing over it. The grey curve in Figure 1a shows the cyclic voltammogram (CV) of SLG/PET electrode in $0.5 \text{ M H}_2\text{SO}_4$ solution recorded in the absence of the Pt

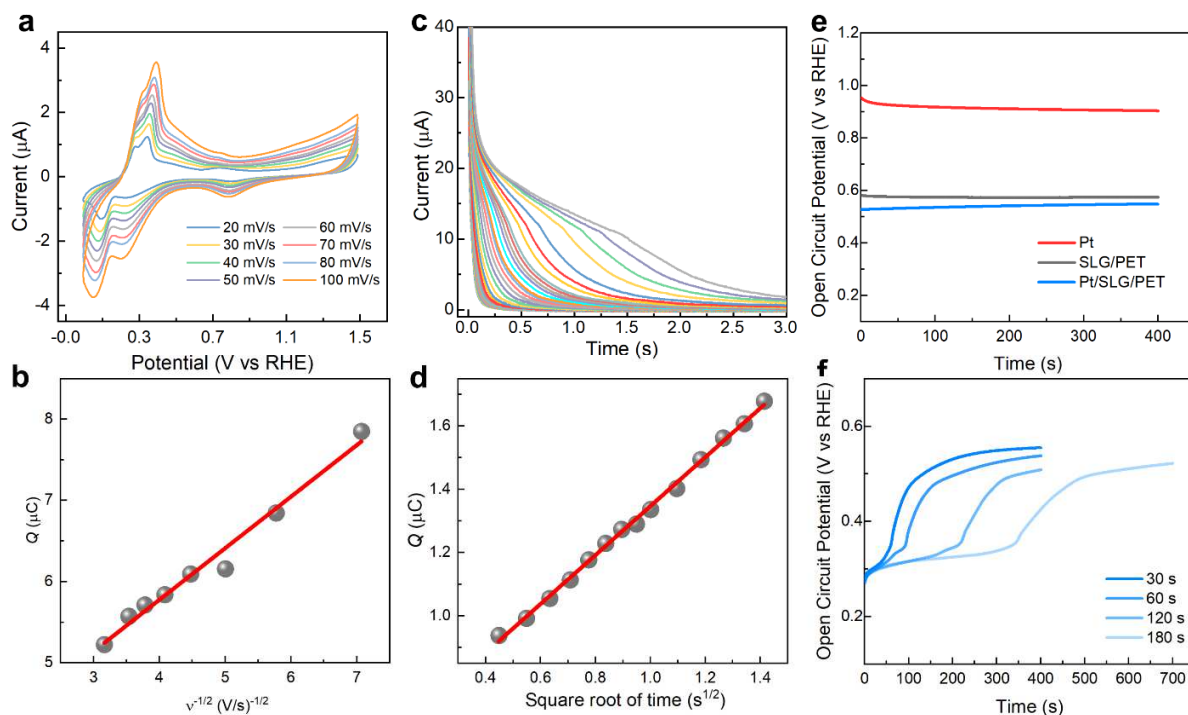


Figure 2. Quantitative measurements of the surface diffusion behaviors of electrodeposited hydrogen adatoms. (a) Cyclic voltammetry of the activated Pt/SLG/PET composite electrode carried out at different scan rates. (b) Linear relationship between the charge of H_{ad} desorption and the reciprocal of the square root of the scan rate. (c) Chronoamperometry of the activated Pt/SLG/PET composite electrode. The electrode potential was held at 0.10 V for 0.1, 0.2, 0.3, 0.4, 0.5, 0.6, 0.7, 0.8, 0.9, 1, 1.2, 1.4, 1.6, 1.8, 2, 2.5, 3, 4, 5, 6, 7, 8, 9, 10, 12, 14, 16, 18, 20, 25, 30, 40, 60, 80, 100, 120 s (from left to right), and then stepped to 0.7 V. (d) Plot of the charge versus square root of time over the shortest [0.2 s~2 s] holding time range. (e) Open circuit potential of the Pt microwire electrode alone (red), SLG/PET electrode (green), and Pt/SLG/PET system (blue). (f) Plots of open circuit potential versus time for the Pt/SLG/PET assembly after it was held at 0.10 V during 30, 60, 120, and 180 s before measuring the open circuit potential. The dimensions of the SLG flake were 4 mm \times 4 mm.

microwire. The CV exhibits the typical SLG capacitive behavior of the formed electric double layer (EDL), as observed on conventional carbon electrodes. The blue curve in Figure 1a is the CV of a Pt/PET electrode in 0.5 M H_2SO_4 solution, which exhibits the classic voltammetric fingerprint of hydrogen adsorption/desorption in the “hydrogen region” [0.05 V, 0.40 V], and that of water dissociation adsorption/desorption in the “oxygen region” [0.50 V, 1.40 V].^{24,25} The red voltammetric scans in Figure 1a show that the Pt/SLG/PET electrochemical assembly exhibits drastically different behavior from that of Pt/PET in the hydrogen adsorption region. In the cathodic scan, the two current peaks corresponding to hydrogen adsorption are asymmetrical and show the characteristics expected for electrochemical mechanisms coupled with mass transfer processes, rather than the simple Faraday adsorption onto a small surface area. In the anodic scan, the desorption potentials of H_{ad} are shifted positively compared with those shown by the blue CV in Figure 1a. Figure S4 shows that the anodic stripping current correlates with the cathodic H_{ad} deposition. Moreover, the two anodic CV peaks overlap, indicating a different desorption mechanism and a higher desorption energy than that measured on Pt/PET electrodes. Note that both the adsorption and desorption currents continue growing during repetitive scans, indicating that they

are under kinetic control. Interestingly, the behavior observed in the oxygen region remains identical to that observed on the Pt/PET electrode. All of the above changes demonstrate that there are important interactions between H_{ad} and SLG (see Figure S1-S3 for more detailed description and analysis).

H_{ad} generated during the cathodic scan is desorbed during the anodic scan in the form of free protons in the electrolyte solution.²⁶ Therefore, the charge obtained from the integrated current of the sharp anodic peak of the red CV in Figure 1a is equivalent to the quantity of H_{ad} (1 e/atom) stored on the Pt/SLG/PET assembly during the cathodic scan. This is far greater than that recorded in the absence of SLG (blue curve in Figure 1a), demonstrating unambiguously that the H_{ad} adsorption capacity of the Pt/SLG/PET assembly electrode greatly exceeds the maximum storage capacity of the Pt microwire alone. Even assuming a high roughness factor of 2, the latter can be estimated to be less than ca. 1 μC , considering the 210 $\mu C/cm^2$ adsorption capacity of polycrystalline Pt.²⁷ This is in contrast with the maximum H_{ad} desorption charge of 19.73 μC obtained at the lowest scan rates (see Figure S7b).

The only reasonable way to explain these numbers is to assume that H atoms electrocatalytically generated by proton electroreduction onto the catalytic surface of the Pt microwire spill over onto the SLG by a surface “site-hopping diffusion/chemisorption” mechanism, as depicted in Figure 1b. Within this framework, considering the 2.1 mm × 1.8 mm dimensions of the SLG flakes used for the determination of loading capacity, the reproducible 19.73 μC maximum charge value indicates a maximum mass ratio of H_{ad} over carbon atoms equal to 6.6 wt%, which corresponds to an effective coverage of ca. 85.7%, i.e., the formation of almost a full monolayer of H_{ad} on SLG (see Figure S7 a and b). These interpretations are thoroughly verified by quantitative investigations based on cyclic voltammetry and chronoamperometry, as discussed below.

Cyclic voltammetry was performed at different scan rates using the activated Pt/SLG/PET electrode immersed in 0.5 M H₂SO₄ solution (Figure 2a). The adsorption of oxygen adspecies at 0.78 V is characterized by a peak current that is proportional to the scan rate (See Figure S5), as expected for adsorption/desorption electrochemical processes. In contrast, the H_{ad}-desorption peak current is proportional to the square root of the scan rate (See Figure S6), which is characteristic of a mass-transfer-limited process. Since this does not occur without an SLG in firm contact with the Pt microwire, it confirms that most of the H_{ad} generated on the Pt electrocatalytic surface spills over onto the SLG surface, which is consistent with the above result showing that the H_{ad} desorption charge is ca. 20 times greater than the storage capacity of the Pt microwire surface. Since the 3.0 mm length of the 25-μm-diameter Pt microwire is much greater than the width of its tangential contact area with the 4 mm × 4 mm SLG flake, H_{ad} site-hopping diffusion on SLG approximately obeys semi-infinite linear diffusion laws for short experimental durations, i.e., provided that the SLG is far from being fully loaded (see more details below in chronoamperometric experiments section). A value of $D = 7.98 \times 10^{-6} \text{ cm}^2 \text{ s}^{-1}$ at 25 °C can be extracted for the apparent surface-diffusion coefficient of H_{ad} on SLG²⁸ from the slope of the linear relationship between the charge (Q) of H_{ad} desorption and the reciprocal of the square root of the scan rate ($v^{-1/2}$) (Figure 2b and see Supporting information (SI) section S1).

Chronoamperometric investigations were performed to further validate the above-mentioned mechanism. The curves performed at 0.7 V after different holding times at 0.1 V in the hydrogen region are shown in Figure 2c. The current was recorded during this desorption process. For holding times longer than 2 s, the desorption i - t curve exhibits a plateau-like region whose duration increases with increasing holding time. This non-classical behavior indicates that, during the unloading (oxidative) phase, the surface concentration of H_{ad} on the Pt microwire surface is almost constant if the holding time was long enough. In other words, the desorption of H_{ad} from the Pt surface due to its oxidation is continuously compensated by a near steady-state flux of H_{ad} flowing back from the SLG surface, where it had been loaded and stored during the holding time duration at 0.1 V. Observation of this behavior requires that the SLG surface is significantly loaded during the cathodic

phase, i.e., sufficiently long charging times (> 2 s for the Pt/SLG/PET assembly used in Figure 2c). For shorter loading times (≤ 2 s), the current plateau is not apparent, and the integrated charge of the H_{ad} desorption peak varies linearly with the square root of the holding time (Figure 2d). A surface diffusion coefficient of H_{ad} on SLG can then be estimated as ca. $D = 1.2 \times 10^{-5} \text{ cm}^2 \text{ s}^{-1}$ (25 °C) from the slope of the linear relationship (Figure 2d and Section S1 in SI), and it is close to that already determined by voltammetry. Finally, a mass ratio of H_{ad} per carbon atom is calculated as 6.2 wt%, i.e., a H_{ad} coverage of 80.5%, is deduced from the maximum charge integral (18.25 μC) releasable after large holding times (Figure S7, c and d) upon using the 2.1 mm × 1.8 mm SLG. All these values are consistent with the results obtained by CV, confirming the validity of the electrocatalytic “spillover-surface diffusion-chemisorption” mechanism.

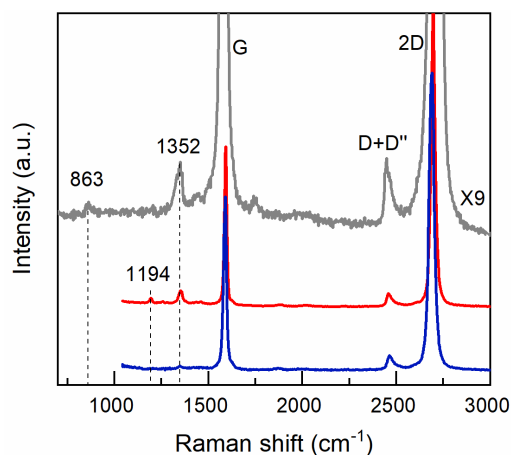


Figure 3. Spectroscopic evidences of the formation of C-H adsorption chemical bonds on graphene. Ex-situ Raman spectra of pristine graphene (blue line), electrochemically activated graphene exhibiting a C-H band at 1194 cm⁻¹ (red line), and deuterium substitution experiment on ultrathin HOPG, exhibiting a C-D band at 863 cm⁻¹ (gray line).

Open circuit potential (OCP) tests were performed to investigate the capacity of the Pt/SLG/PET assemblies to preserve H_{ad}. Before loading the systems, the Pt microwire electrode, the SLG/PET electrode, and the Pt/SLG/PET assembly, showed OCPs of 0.92 V, 0.58 V, and 0.55 V respectively (Figure 2e). After holding the Pt microwire electrode at 0.1 V for various holding times to load H_{ad} onto the Pt/SLG/PET assembly, the OCP was measured again. The OCP-time curves of the loaded Pt/SLG/PET sample show an initial, plateau-like transition feature at ca. 0.3 V before increasing to eventually reach the 0.55 V value observed in the absence of loading (Figure 2f). The duration of this plateau-like transition feature increases with holding time, confirming that this feature corresponds to the non-equilibrium system dynamics, in which H_{ad} stored on SLG diffuses to the Pt/SLG boundary and desorbs from the Pt surface to the electrolyte solution as protons, as the system relaxes its energy via its stray resistances. From all the above electrochemical measurements, it is concluded that the reductive hydrogen adatoms (H_{ad}) generation ($\text{H}^+ + \text{e} \rightarrow \text{H}_{\text{ad}}$) and their oxidative release ($\text{H}_{\text{ad}} \rightarrow \text{H}^+ + \text{e}$) occur on the Pt-wire surface while they

are mostly stored on the SLG surface. Pt performs mostly as an electrocatalyst for each step while SLG, being inert for these electrochemical reactions, offers a large storage capacity. It indicates that H_{ad} adatoms generated at the Pt microwire surface during the cathodic step are spilling over onto SLG and stored onto it.

Raman spectroscopy was used to characterize the graphene surface changes during this process. Before the cathodic loading phase, the G mode (1590 cm^{-1}), the 2D peak (2687 cm^{-1}), and the D+D" peak (2465 cm^{-1}) modes of the pristine SLG were observed (Figure 3, blue curve). After loading, a new Raman mode (Figure 3, red curve) appeared at 1194 cm^{-1} . This new mode is very close to the mode (1184 cm^{-1}) reported previously for catalytic hydrogenation of carbons,²⁹ and it is assigned to a non-covalent C··H vibrational mode of the atomic hydrogen bound directly to the graphene basal plane. If our assignment is correct, the Raman peak at 1194 cm^{-1} should shift to 853 cm^{-1} upon exchanging H with deuterium (D). To test this hypothesis while eliminating background interference from PET or SiO_2 supports, ultrathin HOPG sheets, instead of SLG, were electrochemically loaded in 0.5 M D_2SO_4 solutions. The change of carbon material did not modify the voltammetric behavior (Figure S9a), and the Raman peak at 1194 cm^{-1} shifted down to 863 cm^{-1} (Figure 3 gray curve and Figure S9b). This series of Raman investigations confirm that H_{ad} (or D_{ad}) atoms electrogenerated on the electrocatalytic surface of a Pt microwire can easily spill over onto ultrathin carbon-sheet surfaces through site-hopping diffusion via the formation of stable chemical C··H (or C··D) bonds. Moreover, these Raman spectroscopy experiments indirectly confirmed the stability of these C··H (or C··D) bonds under ambient conditions. Indeed, they were carried out ex-situ, in a Raman spectrophotometer, after disconnecting the electrochemically preloaded HOPG ultrathin sheets from their Pt contacts and removing them from the electrochemical cell. In addition, the enhancement of the D mode at 1352 cm^{-1} (Figure 3, gray curve), which corresponds to the breathing mode of the HOPG six-carbon-atom benzene rings, demonstrates an increase in sp^3 defects,³⁰ indicating that under our conditions, the chemisorption of H_{ad} (or D_{ad}) on SLG preferentially binds to the closed, 6-member rings. Nevertheless, the I_D/I_G ratio were calculated as 0.02 for pristine SLG, 0.08 for H_{ad} -SLG, and 0.03 for D_{ad} -HOPG. According to the evaluation criterion proposed previously³¹, the inter-defect distance (L_D) can be 27 nm or larger. The results show that the spilling and storage of H_{ad} or D_{ad} onto SLG introduce too little sp^3 -defects to change the intrinsic structure of SLG. In summary, we obtained no convincing Raman evidence for the presence of a significant amount of C-H covalent bonds, although the C-H stretch mode of hydrogenated graphene (i.e., graphane) would be observable at 2500 cm^{-1} and 2800 cm^{-1} by IR-vis sum-frequency generation spectroscopy based on previous authors' reports.^{32,33} All these Raman results concur to corroborate the formation of stable C··H adsorption bonds under the present electrochemical conditions.

To gain more insight into the kinetics of the site-hopping surface diffusion of H_{ad} on SLG, the apparent surface diffu-

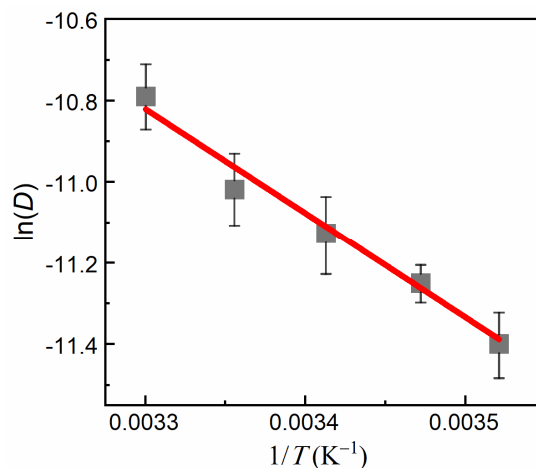


Figure 4. Arrhenius plot of the variation of the apparent surface diffusion coefficient, D , of H_{ad} on SLG with temperature. Values were determined by performing cyclic voltammetry on Pt/SLG/PET assemblies in 0.5 M H_2SO_4 solution (see Figure S10). Error bars indicate standard deviations.

sion coefficients, D , of H_{ad} onto SLG were measured at different temperatures using the $4\text{ mm} \times 4\text{ mm}$ SLG flakes and the voltammetric method detailed above (Figure S10). These results show that the apparent surface diffusion coefficient follows an Arrhenius-type equation (Figure 4 and Section 2 in SI), i.e., $D = D_0 \exp(-\Delta E_a/kT)$, where $D_0 \sim 9.54 \times 10^{-2}\text{ cm}^2\text{ s}^{-1}$ is the pre-exponential factor, and $\Delta E_a \sim 21.34\text{ kJ mol}^{-1}$ (i.e., 0.22 eV per site) is the activation Gibbs free energy associated with jumps between adjacent sites (k is the Boltzmann constant, and T is the absolute temperature).

4. CONCLUSIONS

In conclusion, stable monolayer of atomic hydrogen can be electrodeposited on single layer graphene (SLG) through a Pt-electrocatalyzed “spillover-surface diffusion-chemisorption” mechanism that was established and fully characterized electrochemically. The stability of the chemically adsorbed hydrogen atoms on SLG under ambient conditions was demonstrated by using ex-situ Raman spectroscopy experiments, including H/D isotopic assays for characterizing the existence of C··H or C··D adsorption bonds by their wagging modes. The site-hopping surface diffusion coefficient and the corresponding activation Gibbs free energy were measured as $\sim 10^{-5}\text{ cm}^2\text{ s}^{-1}$ and $\sim 21.34\text{ kJ mol}^{-1}$ (0.22 eV per site), respectively. The adsorption capacity of H_{ad} on SLG under ambient conditions was shown to be 6.6 wt\% , i.e., a coverage greater than 85% , which is higher than the aim for 2025 published by the DOE (5.5 wt\%).³⁴ Since H_2 can be released from the H_{ad} -chemisorbed graphene layers through moderate heating, these results point to the value of the present Pt-electrocatalyzed “spillover-surface diffusion-chemisorption” mechanism on graphene as a very promising hydrogen storage process.

ASSOCIATED CONTENT

Supporting Information.

The Supporting Information is available free of charge at <http://pubs.acs.org>. Supplementary notes of the measurements of the apparent surface diffusion coefficient and activation energy of surface diffusion, more experimental details and Figures S0–S10 are included.

AUTHOR INFORMATION

Corresponding Author

dpzhan@xmu.edu.cn

hanlianhuan@xmu.edu.cn

christian.amatore@ens.psl.eu

Notes

Authors declare that they have no competing interests.

ACKNOWLEDGMENT

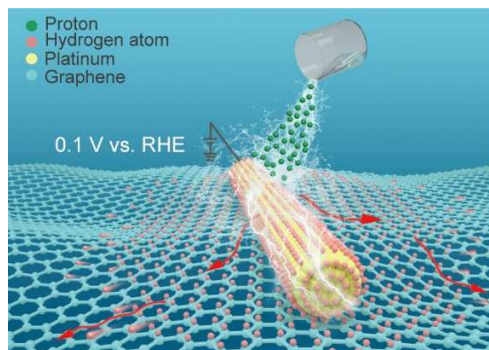
This work was financially supported by the National Natural Science Foundation of China (NSFC 21827802, 22021001). In France, C.A., I.S. and A.O. acknowledge the support from CNRS, ENS - PSL University and Sorbonne University (UMR 8640 PASTEUR). Both national teams as well as the Sino-French LIA CNRS NanoBioCatEchem International Laboratory.

REFERENCES

- (1) Lubitz, W.; Tumas, W. Hydrogen: An Overview. *Chem. Rev.* **2007**, *107* (10), 3900–3903.
- (2) Schlapbach, L.; Züttel, A. Hydrogen-Storage Materials for Mobile Applications. *Nature* **2001**, *414* (6861), 353–358.
- (3) Eberle, U.; Felderhoff, M.; Schüth, F. Chemical and Physical Solutions for Hydrogen Storage. *Angew. Chemie Int. Ed.* **2009**, *48* (36), 6608–6630.
- (4) Dalebrook, A. F.; Gan, W.; Grasmann, M.; Moret, S.; Laurenczy, G. Hydrogen Storage: Beyond Conventional Methods. *Chem. Commun.* **2013**, *49* (78), 8735–8751.
- (5) Bonaccorso, F.; Colombo, L.; Yu, G.; Stoller, M.; Tozzini, V.; Ferrari, A. C.; Ruoff, R. S.; Pellegrini, V. Graphene, Related Two-Dimensional Crystals, and Hybrid Systems for Energy Conversion and Storage. *Science* **2015**, *347* (6217), 1246501.
- (6) Pumera, M. Graphene-Based Nanomaterials for Energy Storage. *Energy Environ. Sci.* **2011**, *4* (3), 668.
- (7) Tozzini, V.; Pellegrini, V. Prospects for Hydrogen Storage in Graphene. *Phys. Chem. Chem. Phys.* **2013**, *15* (1), 80–89.
- (8) Tibbetts, G. G.; Meisner, G. P.; Olk, C. H. Hydrogen Storage Capacity of Carbon Nanotubes, Filaments, and Vapor-Grown Fibers. *Carbon* **2001**, *39* (15), 2291–2301.
- (9) Yang, R. T. Hydrogen Storage by Alkali-Doped Carbon Nanotubes—Revisited. *Carbon* **2000**, *38* (4), 623–626.
- (10) Wang, L.; Yang, R. T. New Sorbents for Hydrogen Storage by Hydrogen Spillover - a Review. *Energy Environ. Sci.* **2008**, *1* (2), 268–279.
- (11) Psogianakis, G. M.; Froudakis, G. E. Fundamental Studies and Perceptions on the Spillover Mechanism for Hydrogen Storage. *Chem. Commun.* **2011**, *47* (28), 7933.
- (12) Gerber, I. C.; Serp, P. A Theory/Experience Description of Support Effects in Carbon-Supported Catalysts. *Chem. Rev.* **2020**, *120* (2), 1250–1349.
- (13) Prins, R. Hydrogen Spillover. Facts and Fiction. *Chem. Rev.* **2012**, *112* (5), 2714–2738.
- (14) Conner, W. C.; Falconer, J. L. Spillover in Heterogeneous Catalysis. *Chem. Rev.* **1995**, *95* (3), 759–788.
- (15) Lin, Y.; Ding, F.; Yakobson, B. I. Hydrogen Storage by Spillover on Graphene as a Phase Nucleation Process. *Phys. Rev. B* **2008**, *78* (4), 041402.
- (16) Cho, E. S.; Ruminski, A. M.; Aloni, S.; Liu, Y.-S.; Guo, J.; Urban, J. J. Graphene Oxide/Metal Nanocrystal Multilaminates as the Atomic Limit for Safe and Selective Hydrogen Storage. *Nat. Commun.* **2016**, *7* (1), 10804.
- (17) Blankenship II, T. S.; Balahmar, N.; Mokaya, R. Oxygen-Rich Microporous Carbons with Exceptional Hydrogen Storage Capacity. *Nat. Commun.* **2017**, *8* (1), 1545.
- (18) Li, Y.; Yang, R. T. Hydrogen Storage in Metal-Organic Frameworks by Bridged Hydrogen Spillover. *J. Am. Chem. Soc.* **2006**, *128* (25), 8136–8137.
- (19) Im, J.; Shin, H.; Jang, H.; Kim, H.; Choi, M. Maximizing the Catalytic Function of Hydrogen Spillover in Platinum-Encapsulated Aluminosilicates with Controlled Nanostructures. *Nat. Commun.* **2014**, *5* (1), 3370.
- (20) Kyriakou, G.; Boucher, M. B.; Jewell, A. D.; Lewis, E. A.; Lawton, T. J.; Baber, A. E.; Tierney, H. L.; Flytzani-Stephanopoulos, M.; Sykes, E. C. H. Isolated Metal Atom Geometries as a Strategy for Selective Heterogeneous Hydrogenations. *Science* **2012**, *335* (6073), 1209–1212.
- (21) Wang, H.; Luo, Q.; Liu, W.; Lin, Y.; Guan, Q.; Zheng, X.; Pan, H.; Zhu, J.; Sun, Z.; Wei, S.; Yang, J.; Lu, J. Quasi Pd1Ni Single-Atom Surface Alloy Catalyst Enables Hydrogenation of Nitriles to Secondary Amines. *Nat. Commun.* **2019**, *10* (1), 1–9.
- (22) Jiang, L.; Liu, K.; Hung, S.-F.; Zhou, L.; Qin, R.; Zhang, Q.; Liu, P.; Gu, L.; Chen, H. M.; Fu, G.; Zheng, N. Facet Engineering Accelerates Spillover Hydrogenation on Highly Diluted Metal Nanocatalysts. *Nat. Nanotechnol.* **2020**, *15* (10), 848–853.
- (23) Merte, L. R.; Peng, G.; Bechstein, R.; Rieboldt, F.; Farberow, C. A.; Grabow, L. C.; Kudernatsch, W.; Wendt, S.; Laegsgaard, E.; Mavrikakis, M.; Besenbacher, F. Water-Mediated Proton Hopping on an Iron Oxide Surface. *Science* **2012**, *336* (6083), 889–893.
- (24) Angerstein-Kozłowska, H.; Conway, B. E.; Sharp, W. B. A. The Real Condition of Electrochemically Oxidized Platinum Surfaces. *J. Electroanal. Chem. Interfacial Electrochem.* **1973**, *43* (1), 9–36.
- (25) Climent, V.; Feliu, J. M. Thirty Years of Platinum Single Crystal Electrochemistry. *J. Solid State Electrochem.* **2011**, *15* (7–8), 1297–1315.
- (26) Zhan, D.; Velmurugan, J.; Mirkin, M. V. Adsorption/Desorption of Hydrogen on Pt Nanoelectrodes: Evidence of Surface Diffusion and Spillover. *J. Am. Chem. Soc.* **2009**, *131* (41), 14756–14760.

- (27) Trasatti, S.; Petrii, O. A. Real Surface Area Measurements in Electrochemistry. *Pure Appl. Chem.* **1991**, *63* (5), 711–734.
- (28) Wang, W.; Zhang, J.; Wang, F.; Mao, B.-W. W.; Zhan, D.; Tian, Z.-Q. Q. Mobility and Reactivity of Oxygen Adspecies on Platinum Surface. *J. Am. Chem. Soc.* **2016**, *138* (29), 9057–9060.
- (29) Liu, X. M.; Tang, Y.; Xu, E. S.; Fitzgibbons, T. C.; Larsen, G. S.; Gutierrez, H. R.; Tseng, H.-H.; Yu, M.-S.; Tsao, C.-S.; Badding, J. V.; Crespi, V. H.; Lueking, A. D. Evidence for Ambient-Temperature Reversible Catalytic Hydrogenation in Pt-Doped Carbons. *Nano Lett.* **2013**, *13* (1), 137–141.
- (30) Ferrari, A. C.; Basko, D. M. Raman Spectroscopy as a Versatile Tool for Studying the Properties of Graphene. *Nat. Nanotechnol.* **2013**, *8* (4), 235–246.
- (31) Cançado, L. G.; Jorio, A.; Ferreira, E. H. M.; Stavale, F.; Achete, C. A.; Capaz, R. B.; Moutinho, M. V. O.; Lombardo, A.; Kulmala, T. S.; Ferrari, A. C. Quantifying Defects in Graphene via Raman Spectroscopy at Different Excitation Energies. *Nano Lett.* **2011**, *11* (8), 3190–3196.
- (32) Alsalem, H.; Just-Baringo, X.; Larrosa, I.; Monteverde, U.; Jiang, X.; Feng, Y.; Koehler, S. P. K. Evidence for Site-Specific Reversible Hydrogen Adsorption on Graphene by Sum-Frequency Generation Spectroscopy and Density Functional Theory. *J. Phys. Chem. C* **2019**, *123* (42), 25883–25889.
- (33) Kim, H.; Balgar, T.; Hasselbrink, E. The Stretching Vibration of Hydrogen Adsorbed on Epitaxial Graphene Studied by Sum-Frequency Generation Spectroscopy. *Chem. Phys. Lett.* **2011**, *508* (1–3), 1–5.
- (34) Available at <https://www.energy.gov/eere/fuelcells/downloads/target-explanation-document-onboard-hydrogen-storage-light-duty-fuel-cell>. (accessed May 2021)

TOC



Pt-assisted electrochemical storage of atomic hydrogen on single layer graphene at ambient conditions easily reaches the theoretical loading limit.